

Electronic Supporting Information

Solid-State Coexistence of {Zr₁₂} and {Zr₆} Zirconium Oxocarboxylate Clusters

Iurie L. Malaestean, Meliha Kutluca Alıcı, Claire Besson, Arkady Ellern and Paul Kögerler*

Crystallographic Details

The carboxylate ligands in compounds **1** and **2** are highly disordered; therefore similarity restraints (SIMU, DELU, SADI) were applied to obtain reasonable geometrical parameters and thermal displacement coefficients. However, even after applications of those restraints some ADPs for Oxo-carboxylate ligands which is very typical for this family of clusters. In structure **1** one of the butyl groups was found disordered by two positions with occupancy factor 0.5. The crystal structure of **1** also has huge voids accessible for solvents but not all of them were objectively located on a difference Fourier map and refined. The attempt to apply the SQUEEZE routine [A. L. Spek, *J. Appl. Cryst.*, 2003, **36**, 7] designed to treat electron density of disordered and diffused solvents did not result in any improvement; therefore the original datasets were used for the final refinements. All calculations were performed using BRUKER APEX II software suite [Bruker AXS Inc., Madison, Wisconsin, USA].

Note that we were unable to obtain crystals of the ZrCl₄-derived precursor compound [Zr₆O₄(OH)₄(pr)₁₂]₂·6Hpr (see below) suitable for single-crystal X-ray diffraction analysis.

Table S1. Summary of crystallographic details, data collection, and refinement details for **1** and **2**

Compound	1	2
Empirical Formula	C ₁₇₄ H ₂₈₇ Co ₈ N ₂₁ O ₁₁₉ Zr ₁₈	C ₁₂₀ H ₁₈₀ Co ₆ N ₆ O ₅₀ Zr ₆
Formula weight / g mol ⁻¹	6690.63	3407.6
T / K	173(2)	173(2)
λ / Å	0.71073	0.71073
Crystal system	monoclinic	hexagonal
Space group	C2/c	P6 ₃ 22
a / Å	36.819(4)	18.423(5)
b / Å	31.046(3)	18.423(5)
c / Å	28.384(5)	26.934(7)
α	90°	90°
β	123.688(1)°	90°
γ	90°	120°
V / Å ³	26996(6)	7917(4)
Z	4	2
D _{calc} / g cm ⁻³	1.646	1.429
μ / mm ⁻¹	1.230	1.064
F(000)	13464	3488
θ range for data collection	0.93° – 28.32°	1.28° – 21.00°
Index ranges	–49 ≤ h ≤ 49, –41 ≤ k ≤ 41, –37 ≤ l ≤ 37	–18 ≤ h ≤ 18, –18 ≤ k ≤ 18, –27 ≤ l ≤ 27
Absorption corrections (T _{min} / T _{max})	0.76 / 0.85	0.78 / 0.90
Reflections collected	97371	42012
Completeness to θ _{max}	99.9%	98.0%
Data / restraints / parameters	21198 / 735 / 1568	2815 / 156 / 271
Final R indices [I > 2σ(I)]	R ₁ = 0.0752, wR ₂ = 0.1916	R ₁ = 0.0850, wR ₂ = 0.2102
R indices (all data)	R ₁ = 0.1198, wR ₂ = 0.2613	R ₁ = 0.0855, wR ₂ = 0.2106
Goodness-of-fit (GOF) on F ²	1.100	1.232

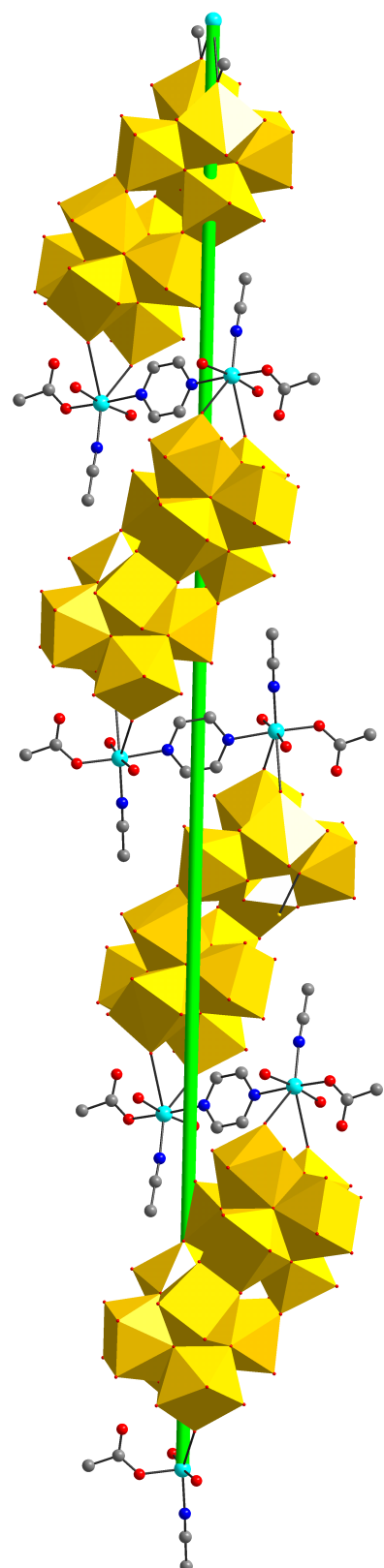


Fig. S1 Schematic simplified representation of the helical structure of the $\{\text{Zr}_{12}\}$ -based coordination polymer **A** in compound **1** and its propagation axis (green).

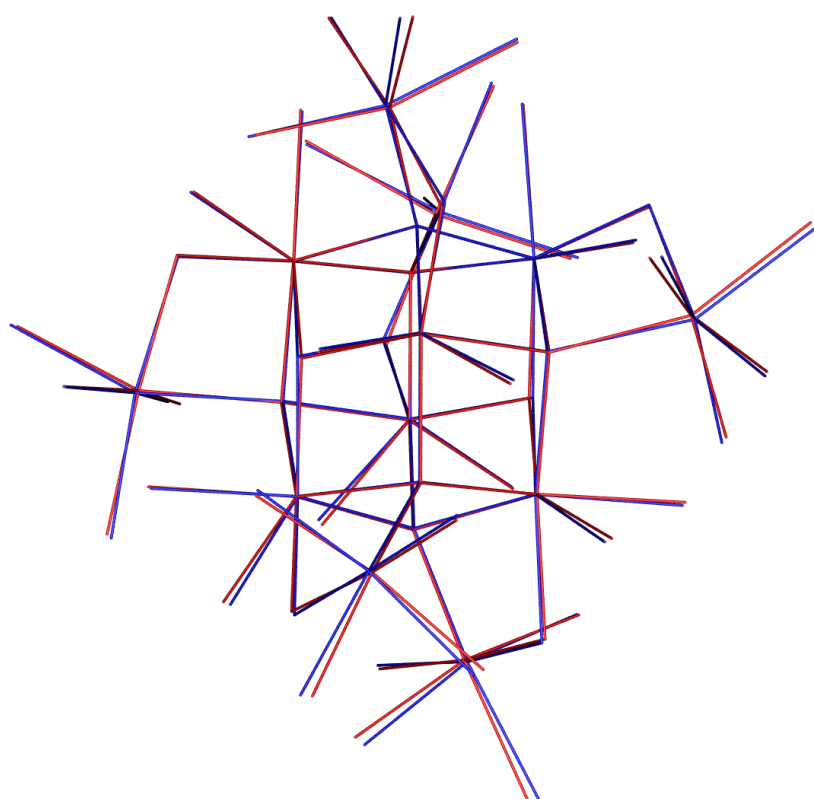


Fig. S2 Overlay of the core $\{\text{Co}_6\text{Zr}_6\}$ geometries: complex **B** in compound **1** (blue) and the corresponding structure in compound **2** (red). Only the Co and Zr coordination environments are shown, H and C omitted.

Synthesis of the precursor $[\text{Zr}_6\text{O}_4(\text{OH})_4(\text{pr})_{12}]_2 \cdot 6\text{Hpr}$

We noticed that the reproducible synthesis of compounds **1** and **2** required two different synthesis routes for the precursor compound $[\text{Zr}_6\text{O}_4(\text{OH})_4(\text{pr})_{12}]_2 \cdot 6\text{Hpr}$, which we postulate to be caused by small amounts of starting reagents that are present in the microcrystalline products. Whereas synthesis of **1** required the use of the precursor synthesized as described in ref. 5 (reacting $\text{Zr}(\text{OBu})_4$ with propionic acid at room temperature), synthesis of **2** required the precursor to be synthesized using a different protocol: ZrCl_4 (2.0 g, 8.58 mmol) was heated for 4 h in 10.0 mL (133.7 mmol) propionic acid. The thus-obtained microcrystalline product was filtered off, washed with pentane and dried in air (yield: 2.12 g, 82% based on Zr). Elemental analysis, calcd. (found) for $\text{C}_{90}\text{H}_{164}\text{O}_{76}\text{Zr}_{12}$: C, 30.4 (30.13); H, 4.65 (4.76)%. IR data (KBr, ν / cm^{-1}): 3392 br/s, 2980 w, 2942 w, 1718 w, 1545 s, 1469 s, 1440 s, 1375 m, 1302 s, 1212 w, 1080 m, 1014 m, 912 w, 883 w, 810 m, 647 s, 470 m. ESI-MS⁺ (MeOH; ThermoFisher Scientific LTQ-Orbitrap XL): $m/z = 1432$, $\{\text{Zr}_6\text{O}_4(\text{OH})_4(\text{pr})_{10}(\text{MeO})\}^+$, 100%; 1524, $\{\text{Zr}_6\text{O}_4(\text{OH})_4(\text{pr})_{11}(\text{MeOH})(\text{H}_2\text{O})\}^+$, 55%; 2660, $\{\text{Zr}_{12}\text{O}_{16}(\text{pr})_{15}(\text{Hpr})_2(\text{CH}_3\text{OH})_2(\text{H}_2\text{O})\}^+$, 15%.

¹H-NMR (in deuterated toluene; Bruker Ultrashield Plus 400; Fig. S3) allowed us to identify the product as a dimeric [Zr₆O₄(OH)₄(pr)₁₂]₂ species, and not a monomeric [Zr₆O₄(OH)₄(pr)₁₂] species, cmp. Fig. 9 in ref. 5.

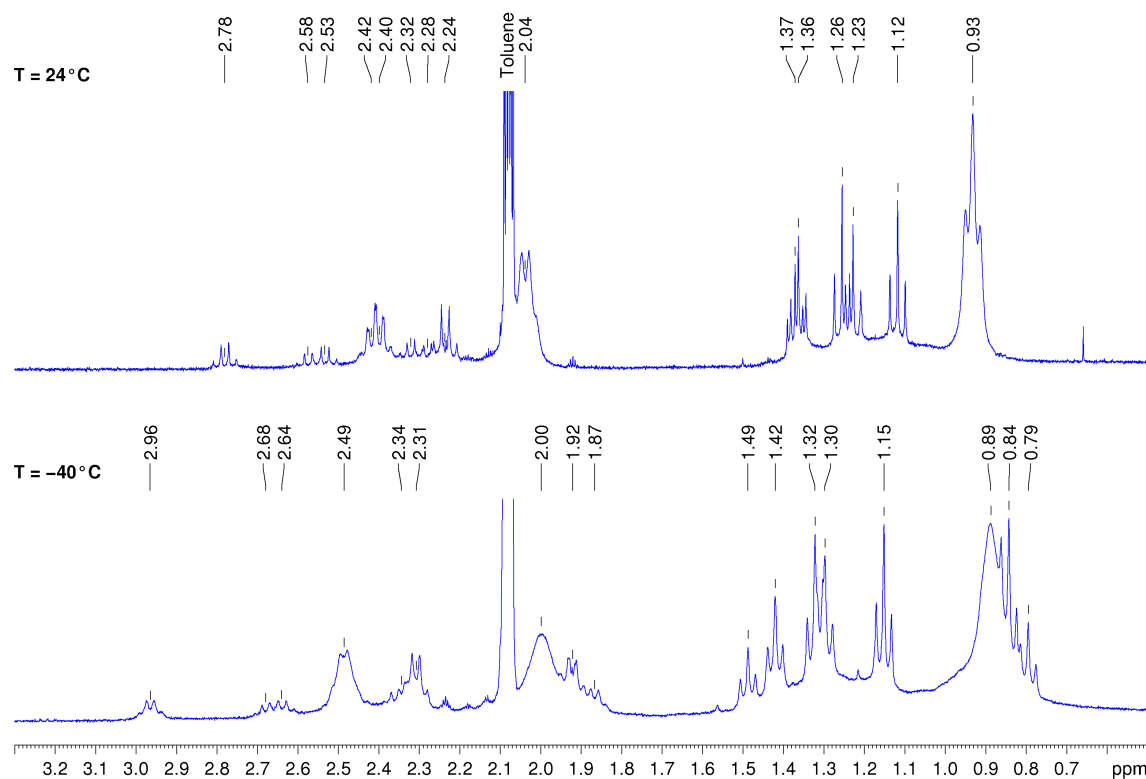


Fig. S3 ¹H-NMR of the ZrCl₄-derived precursor [Zr₆O₄(OH)₄(pr)₁₂]₂·6Hpr in d₈-toluene.

IR spectroscopy and thermal stability studies

IR spectra (4000–400 cm⁻¹) were recorded with a Perkin-Elmer Spectrum One spectrometer using KBr pellets. The spectra of complexes **1** and **2** display strong and broad bands in the 1627–1568 and 1439–1438 cm⁻¹ regions that are assigned to the asymmetric and symmetric vibrations of the coordinated carboxylic groups. Strong bands in both complexes at 2973–2966 cm⁻¹ and bands at 1502–1469 cm⁻¹ are assigned to characteristic v(C–H) stretching and bending modes. A medium peak in compound **1** at 1628 cm⁻¹ shows the presence of monodentate carboxylate groups [R. C. Mehrotra, R. Bohra, *Metal Carboxylates*, Academic Press, New York, 1983; K. Nakamoto, *Infrared and Raman Spectra of Inorganic and Coordination Compounds*, 4th ed., Wiley, New York, 1986]. Thermogravimetric and differential thermoanalysis measurements in the 25–600 °C range were performed using a Mettler Toledo TGA/SDTA851 under dry N₂ flux (60 mL/min) at a heating rate of 10 K/min. TGA/DTA graphs of both **1** and **2** (Figs. S4/S5) display endothermic decomposition steps. For **1** three undefined mass loss steps are observed. At 520 °C the observed total weight loss of 50.8% compares to a 49.9% decrease calculated for the loss of eight CH₃CN as solvate

molecules and two coordinated CH_3CN , three NO_3^- groups, one pyrazine molecule, all coordinated propionic acid ligands, and two bda.

Compound **2** shows two weakly defined steps up to 250 °C, where the first step likely corresponds to the decomposition of two biphenol molecules (calcd. 10.9%, found 11.1%). The loss of 12 coordinated propionates, two bda ligands and one biphenol group is observed at 580 °C (calcd. 35.9%, found 39.5%).

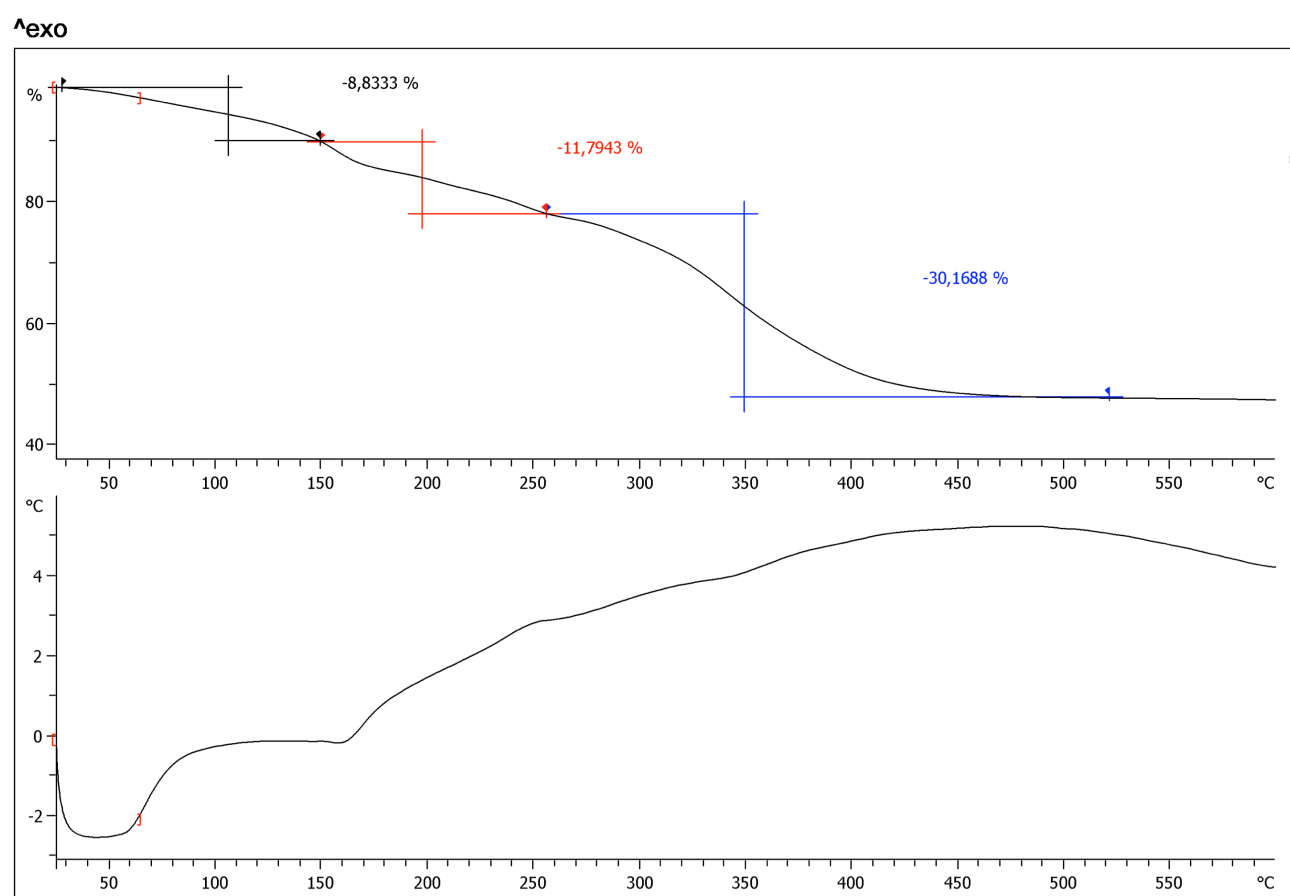


Fig. S4 TGA (top) and DTA (bottom) graphs for compound **1**.

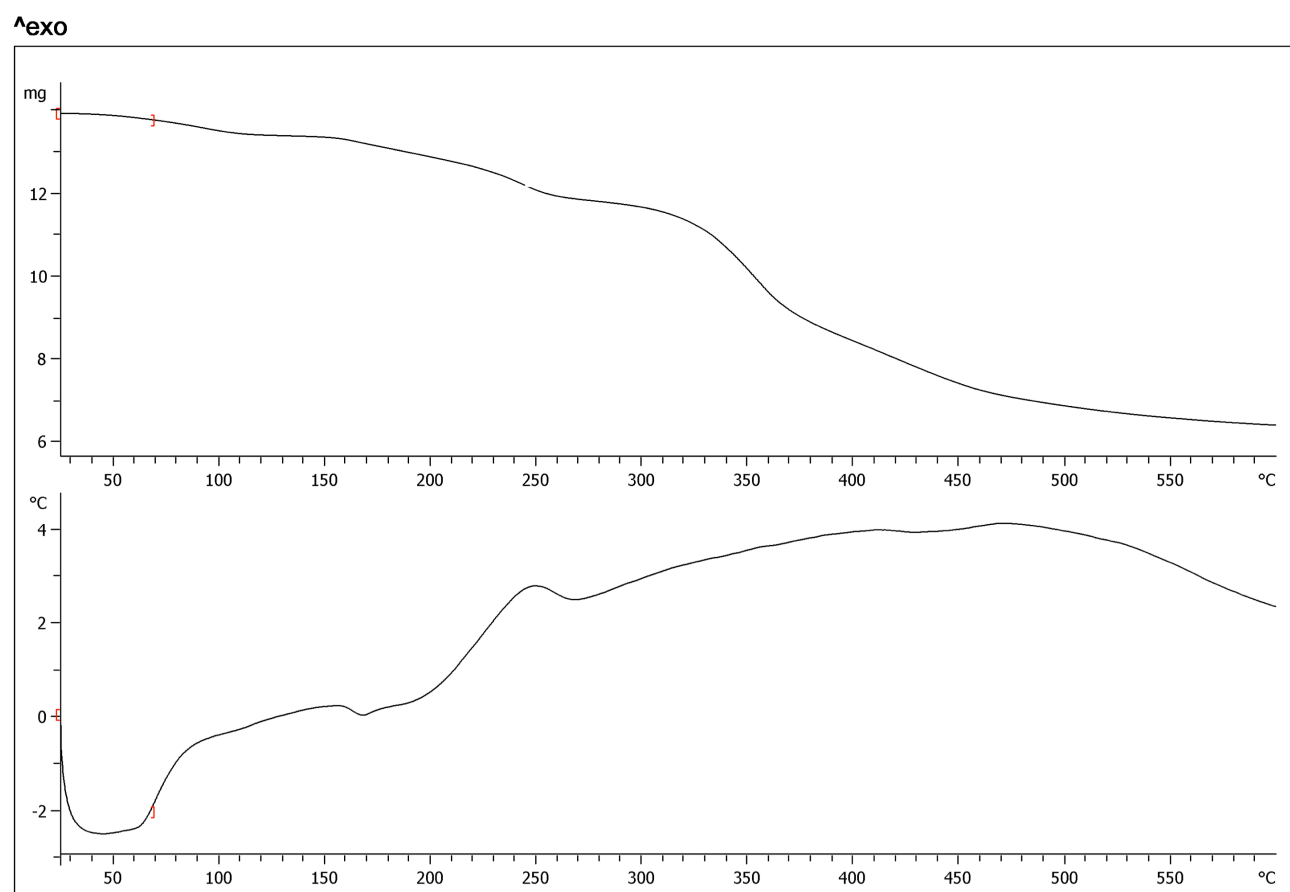


Fig. S5 TGA (top) and DTA (bottom) graphs for compound **2**.